

Supporting Information

Biomass-derived B/N/P co-doped porous carbons as bifunctional materials for supercapacitors and sodium-ion batteries

Yanjiao Li,^a Xufei Zou,^a Shiqi Li,^a Yingying Chen,^{*ab} Guoxiu Wang,^b Hongxun Yang,^{*a} and Hao Tian^{*b}

^a School of Environmental and Chemical Engineering, Jiangsu University of Science and Technology, Zhenjiang 212003, Jiangsu, China

^b Centre for Clean Energy Technology, School of Mathematical and Physical Sciences, Faculty of Science, University of Technology Sydney, Broadway, NSW 2007, Australia.

*Corresponding author.

Email: scyyh@just.edu.cn (Y. Chen); yhongxun@126.com (H. Yang); hao.tian@uts.edu.au (H. Tian)

Text S1

From the GCD results, the specific capacitance (C_s , $F\ g^{-1}$) of the three-electrode system was calculated according to the following equation S2 (Eq. S2) [1]:

$$C_s = \frac{I \times \Delta t}{m \times \Delta V} \quad (S2)$$

The single electrode specific capacitance of the whole symmetric supercapacitors was obtained by the equation S3 (Eq. S3) [1]:

$$C_{cell} = \frac{4 \times I \times \Delta t}{M \times \Delta V} \quad (S3)$$

In which two-electrode systems, the energy density (E , $Wh\ kg^{-1}$) and power density (P , $W\ kg^{-1}$) were calculated by the equations S4 and S5 (Eq. S4 and Eq. S5) [1]:

$$E = \frac{\Delta V^2 C_{cell}}{8 \times 3.6} \quad (S4)$$

$$P = \frac{3600 \times E}{\Delta t} \quad (S5)$$

Where C_s or C_{cell} ($F\ g^{-1}$) is the gravimetric specific capacitance of active materials, I (A) represent the constant discharging current, Δt (s) corresponds to the discharge time, M (g) is the total mass of the positive and negative electrodes and ΔV (V) is the voltage change within discharge process.

The interlayer distance (d_{002}) was calculated using the (002) graphite diffraction peak and Bragg Eq. (S6) [4]:

$$d_{002} = \frac{\lambda}{2 \sin \theta} \quad (S6)$$

where λ is the X-ray wavelength (0.154 nm) and θ is the scattering angle corresponding to the peak position.

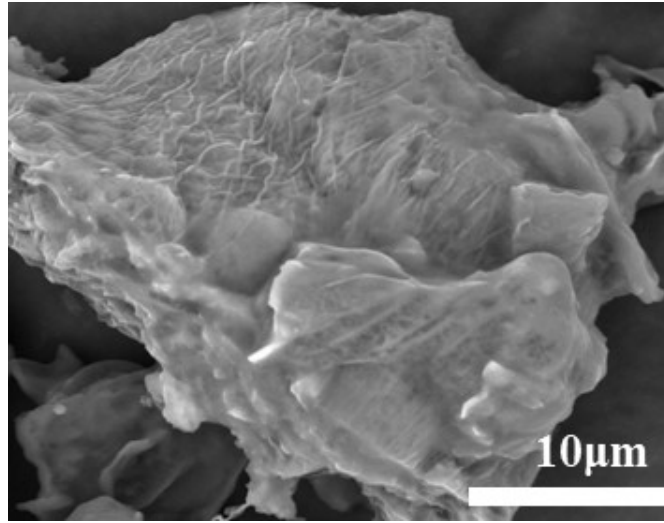


Fig. S1 The original SEM image of OP.

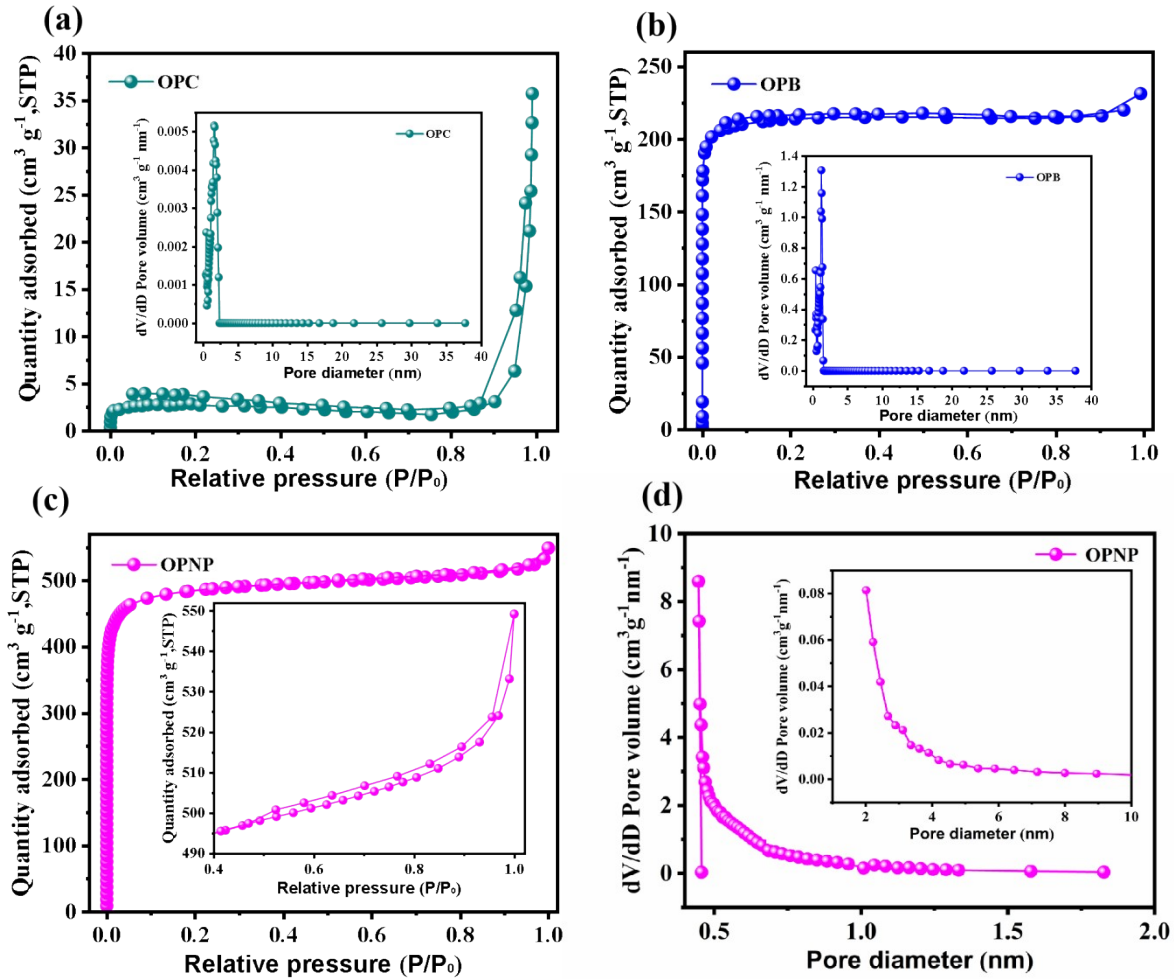


Fig. S2 (a) N_2 adsorption-desorption isotherms of OPC, inset: pore size distribution; (b) N_2 adsorption-desorption isotherms of OPB, inset: pore size distribution; (c) N_2 adsorption-desorption isotherms of OPNP, inset: partial amplification region; (d) the pore size distribution of OPNP.

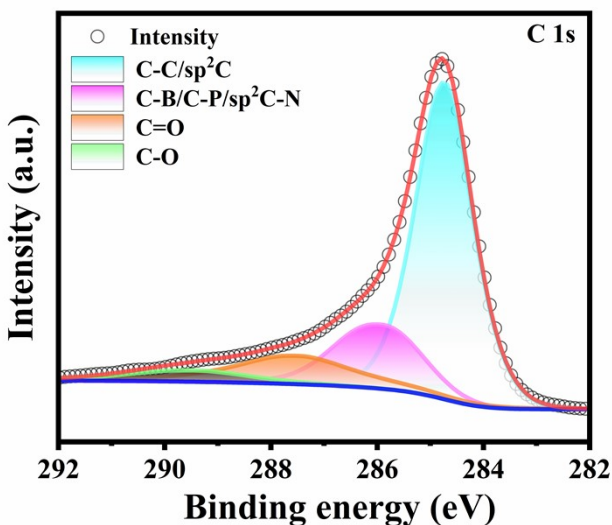


Fig. S3 C 1s high resolution spectra of OPBNP.

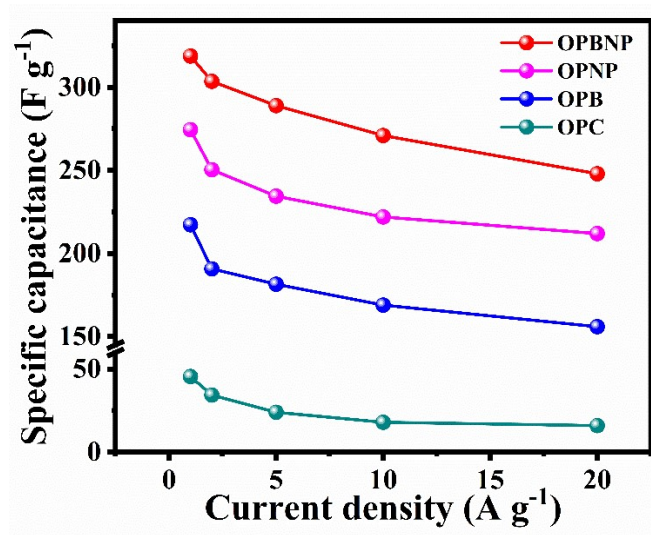


Fig. S4 The OPC, OPB, OPNP, OPBNP specific capacitance values at different current densities.

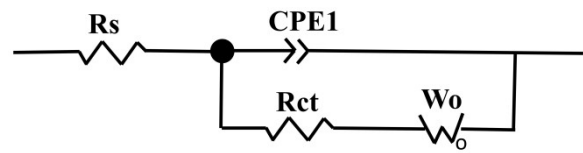


Fig. S5 Equivalent circuit diagram of electrodes.

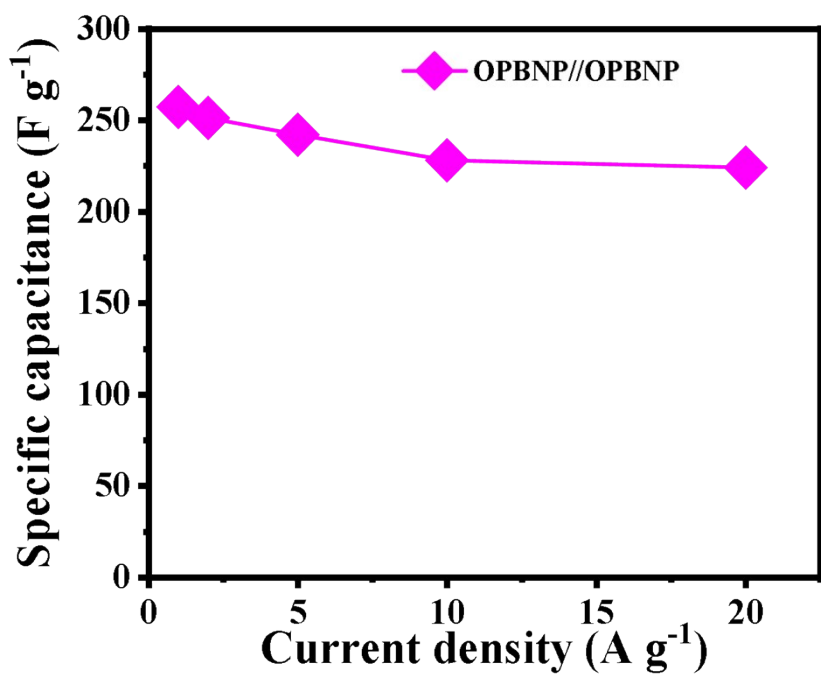


Fig. S6 Specific capacitance at different current densities.

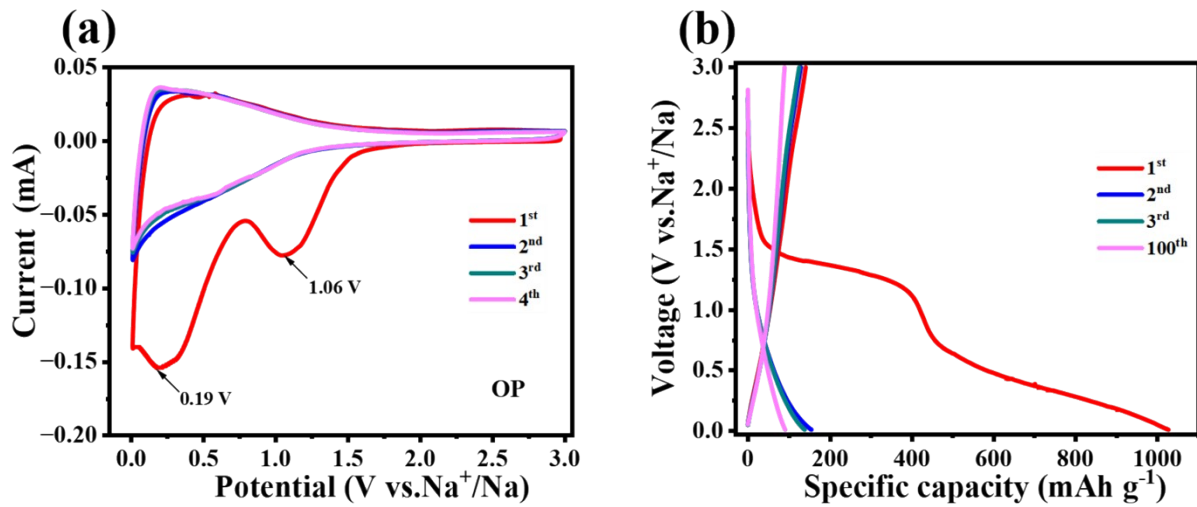


Fig. S7 CV curves of OPC electrodes (a) 0.1 mV s^{-1} ; (b) The charge-discharge curves of the 1st, 2nd, 3rd and 100th cycles at 0.1 A g^{-1} .

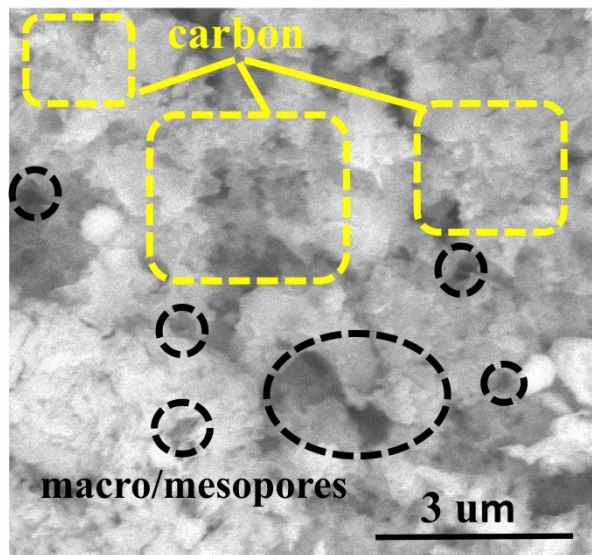


Fig. S8 SEM image of the OPBNP electrode after 1000 cycles at 1 A g^{-1} for SIBs.

Table S1 Results of charge-discharge specific capacitance and impedance parameters of three-electrode system at different current densities.

Current density (A g ⁻¹)	Specific capacitance (F g ⁻¹)			
	OPC	OPB	OPNP	OPBNP
1	45.5	217.3	274.5	318.8
2	34.4	190.8	250.4	303.6
5	24.0	181.5	234.5	289.0
10	18	169.0	222.0	271.0
20	16	156.0	212.0	248.0
Efficiency (%)	35.2	71.7	77.2	77.8
Impedance (Ω)	R_s	0.55	0.61	0.60
	R_{ct}	0.092	0.062	0.053
				0.043

Table S2 Comparisons of specific capacitance (Cs) of nitrogen, phosphorus and other heteroatomic co-doped biomass-derived carbon.

Carbon source	Activation method	S _{BET} (m ² g ⁻¹)	Cs (F g ⁻¹)	Measurement condition	Refs
Pomelo peel	Thermal + (NH ₄) ₂ HPO ₄	807	240	2 M KOH, 0.5 A g ⁻¹	[5]
shrimp shell	H ₃ PO ₄	726	260	6 M KOH, 0.05 A g ⁻¹	[6]
Walnut shell	KOH+H ₃ PO ₄	2583	332	6 M KOH, 1 A g ⁻¹	[7]
Silkworm cocoon	Phytic acid	1247.2	317	1 M H ₂ SO ₄ , 1 A g ⁻¹	[8]
Bacterial cellulose	(NH ₄) ₂ HPO ₄	731.9	232	6 M KOH, 1 A g ⁻¹	[9]
Molasses	Ammonium polyphosphate	422.9	160	6 M KOH, 1 A g ⁻¹	[10]
Tea leaves		129	158		
Duck weed	KOH	1636	315.2	6 M KOH, 1 A g ⁻¹	[11]
Cicada molasses	KOH	1676	355	6 M KOH, 1 A g ⁻¹	[12]
Orange peel	(NH ₄) ₂ HPO ₄ + Boric acid	1774.8	318.8	6 M KOH, 1 A g ⁻¹	This work

Table S3 Comparisons of the electrochemical performances of biomass-derived hard carbon for SIBs.

Biomass precursor	Calcination temperature e (°C)	current density (A g ⁻¹)	Reversible capacity (mA h g ⁻¹)	Rate (A g ⁻¹)	Reversible capacity (mA h g ⁻¹)	Refs
Coconut			270 (100 cycles)	—	—	[1]
Silk			273 (100 cycles)	—	—	
Walnut shell	1000	0.1	305 (200 cycles)	1	182 (1500 cycles)	[13]
Rice husk	1200	0.025	328.4 (100 cycles)	0.1	232.3 (400 cycles)	[14]
Gelatin medicine residue	700 800	0.2 0.1	309 (200 cycles) 801 (500 cycles)	1 5	225 (2000 cycles) 402 (500 cycles)	[15] [16]
crab shell	800	0.03	339.1 (1 st)	0.5	132.4 (200 cycles)	[17]
Reed straw	1300	0.025	372.0 (1 st)	0.1	283.8 (200 cycles)	[18]
Mushroom stalk	900	0.1	305 (10 cycles)	—	—	[19]
Cirsium setosum	700	0.1	268 (100 cycles)	1	198.6 (320 cycles)	[20]
Mango peel	800	0.1	358 (300 cycles)	2	155 (2500 cycles)	[21]
Orange peel	600	0.1	292.3 (100 cycles)	1	205.1 (1000 cycles)	This work

Table S4 Electrochemical impedance parameters of OPC and OPBNP electrodes

Sample	Impedance (Ω)	
	Rs	Rct
OPC	4.1	291.8
OPBNP	3.2	72.4

References

- 1 L. Tang, Y. B. Zhou, X. Y. Zhou, Y. R. Chai, Q. J. Zheng and D. M. Lin, Enhancement in electrochemical performance of nitrogen-doped hierarchical porous carbon-based supercapacitor by optimizing activation temperature, *J. Mater. Sci.*, 2019, **30**, 2600-2609.
- 2 L. H. Cao, H. L. Li, Z. X. Xu, H. J. Zhang, L. H. Ding, S. Q. Wang, G. Y. Zhang, H. Q. Hou, W. H. Xu, F. Yang and S. H. Jiang, Comparison of the heteroatoms-doped biomass-derived carbon prepared by one-step nitrogen-containing activator for high performance supercapacitor, *Diam. Relat. Mater.*, 2021, **114**, 108316.
- 3 G. Y. Zhao, D. F. Yu, C. Chen, L. Sun, C. H. Yang, H. Zhang, B. S. Du, F. F. Sun, Y. Sun and M. Yu, One-step production of carbon nanocages for supercapacitors and sodium-ion batteries, *J. Electroanal. Chem.*, 2020, **878**, 114551.
- 4 C. Nita, B. Zhang, J. Dentzer and C. M. Ghimbeu, Hard carbon derived from coconut shells, walnut shells, and corn silk biomass waste exhibiting high capacity for Na-ion batteries, *J. Energy. Chem.*, 2021, **58**, 207-218.
- 5 Z. Wang, Y. T. Tan, Y. L. Yang, X. N. Zhao, Y. Liu, L. Y. Niu, B. Tichnell, L. B. Kong, L. Kang, Z. Liu and F. Ran, Pomelo peels-derived porous activated carbon microsheets dual-doped with nitrogen and phosphorus for high performance electrochemical capacitors, *J. Power Sources.*, 2018, **378**, 499-510.
- 6 J. Y. Qu, C. Geng, S. Y. Lv, G. H. Shao, S. Y. Ma and M. B. Wu, Nitrogen, oxygen and phosphorus decorated porous carbons derived from shrimp shells for supercapacitors, *Electrochim. Acta.*, 2015, **176**, 982-988.
- 7 X. L. Su, J. R. Chen, G. P. Zheng, J. H. Yang, X. X. Guan, P. Liu and X. C. Zheng, Three-dimensional porous activated carbon derived from loofah sponge biomass for supercapacitor applications, *Applied Surface Science.*, 2018, **436**, 327-336.
- 8 Y. K. Wang, M. K. Zhang, Y. Dai, H. Q. Wang, H. Y. Zhang, Q. Q. Wang, W. B. Hou, H. Yan, W. R. Li and J. C. Zheng, Nitrogen and phosphorus co-doped silkworm-cocoon-based self-activated porous carbon for high performance supercapacitors, *J. Power Sources*, 2019, **438**, 227045.
- 9 D. B. Kong, L. Cao, Z. M. Fang, F. L. Lai, Z. D. Lin, P. Zhang and Wei Li, Low-cost high-performance asymmetric supercapacitors based on ribbon-like Ni(OH)₂ and biomass carbon nanofibers enriched with nitrogen and phosphorus, *Ionics*, 2019, **25**, 4341-4350.
- 10 S. Macchi, N. Siraj, F. Watanabe and T. Viswanathan, Renewable-resource-based waste materials for supercapacitor application, *Chemistry Select.*, 2019, **4**, 492-501.

- 11 T. Wang, J. Z. Zhang, Q. H. Hou and S. Wang, Utilization of nutrient rich duckweed to create N, P Co-doped porous carbons for high performance supercapacitors, *J. Alloys Compd.*, 2019, **771**, 1009-1017.
- 12 H. Y. Jia, J. W. Sun, X. Xie, K. B. Yin and L. T. Sun, Cicada slough-derived heteroatom incorporated porous carbon for supercapacitor: Ultra-high gravimetric capacitance, *Carbon*, 2019, **143**, 309-317.
- 13 Q. Li, Y. N. Zhang, S. A. Feng, D. Liu, G. X. Wang, Q. L. Tan, S. T. Jiang and J. J. Yuan, N, S self-doped porous carbon with enlarged interlayer distance as anode for high performance sodium ion batteries. *Int. J. Energy. Res.*, 2021, **45**, 7082-7092.
- 14 L. Li, M. F. Sun, Z. Z. Xu, Z. Wang, K. Liu, Y. Y. Chen, Z. Wang, H. Chen and H. X. Yang, Hierarchical porous hard carbon derived from rice husks for high-performance sodium ion storage, *Colloid Surface A.*, 2023, **661**, 130927.
- 15 Q. Z. Jin, W. Li, K. L. Wang, H. M. Li, P. Y. Feng, Z. C. Zhang, W. Wang and K. Jiang, Tailoring 2D heteroatom-doped carbon nanosheets with dominated pseudocapacitive behaviors enabling fast and high-performance sodium storage, *Adv. Funct. Mater.*, 2020, **30**, 1909907.
- 16 H. R. Wan, X. R. Shen, H. Jiang, C. Zhang, K. L. Jiang, T. Chen, L. L. Shi, L. M. Dong, C. C. He, Y. Xu, J. Li and Y. Chen, Biomass-derived N/S dual-doped porous hard-carbon as high-capacity anodes for lithium/sodium ions batteries, *Energy*, 2021, **231**, 121102.
- 17 X. X. Xue, Y. jJ. Weng, Z. D. Jiang, S. C. Yang, Y. K. Wu, S. H. Meng, C. X. Zhang, Q. Sun and Y. L. Zhang, Naturally nitrogen-doped porous carbon derived from waste crab shell as anode material for high performance sodium-ion battery. *J. Anal. Appl. Pyrol.*, 2021, **157**, 105215.
- 18 J. Wang, L. Yan, Q. J. Ren, L. L. Fan, F. M. Zhang and Z. Q. Shi, Facile hydrothermal treatment route of reed straw-derived hard carbon for high performance sodium ion battery. *Electrochim. Acta.*, 2018, **29**, 188-196.
- 19 P. F. Yu, W. C. Zhang, Y. H. Yang, M. T. Zheng, H. Hu, Y. Xiao, Y. L. Liu and Y. R. Liang, Facile construction of uniform ultramicropores in porous carbon for advanced sodium-ion battery. *J. Colloid Interf. Sci.*, 2021, **582**, 852-858.
- 20 L. Y. Cao, Y. Wang, H. L. Hu, J. F. Huang, L. J. Kou, Z. W. Xu and J. Y. Li, N/S co-doped disordered carbon with enlarged interlayer distance derived from cirsium setosum as high-performance anode for sodium ion batteries. *J. Mater. Sci. Mater El.*, 2019, **30**, 21323-21331.
- 21 R. Muruganantham, F. M. Wang and W. R. Liu, A green route N, S-doped hard carbon derived from fruit-peel biomass waste as an anode material for rechargeable sodium-ion storage

applications. *Electrochim. Acta.*, 2022, **424**, 140573.